Bull Mater Sci (2020)43:302
https://doi.org/10.1007/s12034-020-02295-0

Deciphering the role of amine in amino silane-functionalized Pd/rGO catalyst for formic acid decomposition at room temperature

S SMITA BISWAS, M SRI TANDRAPADU, E ABINAYA and M ESWARAMOORTHY*
Nanomaterials and Catalysis Laboratory, Chemistry and Physics of Materials Science, Jawaharlal Nehru Centre for Advanced Scientific Research, Bengaluru 560064, India
*Author for correspondence (eswar@jncasr.ac.in)

MS received 25 January 2020; accepted 27 July 2020

Abstract. Additive free, selective decomposition of formic acid to hydrogen and carbon dioxide at room temperature is still a challenging catalytic process which often requires noble metal catalyst (Pd, AuPd, AuPt) and sodium formate as an additive. Till date, catalyst design is targeted towards minimum noble metal usage along with incorporation of basic functionalities to produce *in situ* formate ion (key intermediate for dehydrogenation) from formic acid. In this work, we have studied the catalytic behaviour of amino silane-functionalized graphene oxide (GO) containing palladium nanoparticles for formic acid decomposition in ambient condition. By varying amine functionalization on GO and palladium content, the best performing catalyst was obtained with 5 wt% palladium loading. Additionally, it was observed for the first time that along with stability of a catalyst in reaction medium, its interaction with decomposed products, i.e., carbon dioxide with amine functional groups plays a crucial role in recyclability of a catalyst.

Keywords. Formic acid; recyclability; graphene oxide; amino silane; palladium; dehydrogenation.

1. Introduction

Hydrogen being a CO_2 neutral energy carrier and a clean alternative to fossil fuel is largely used in fuel cell-based technology. Although its gravimetric energy density is three times higher than gasoline, the low volumetric energy density ($\sim$10 kJ l^{-1} at ambient conditions) makes it ill-suited for a large scale energy storage and transportation. As the production of hydrogen through renewable energy sources is gaining momentum, its efficient storage still remains a key challenge to realize a hydrogen-based energy economy [1]. Conventional physical methods of using high pressure and cryogenic containers to store hydrogen suffer from efficiency and safety problems [2]. The solid hydrogen carriers like zeolites, MOFs, porous carbons and metal hydrides ($NaAlH_4$, MgH_2, etc.), on the other hand, depend on high desorption temperature and/or very low adsorption and storage temperature restricting their wider usage [3–5]. The liquid organic hydrogen carriers (LOHC) for their convenience in transportation, refueling and handling are being considered as potential candidates for hydrogen storage and release. Nevertheless, toxicity, flammability and explosive nature, limits the usage of many LOHCs, such as carbazole derivatives, hydrazine and methyl-cyclohexane [6–8]. Recently, formic acid, holding 4.4 wt% of H_2, is recognized as a stable, non-toxic, biodegradable, liquid hydrogen carrier. It is majorly derived from biomass oxidation and its hydrogenation–dehydrogenation cycle makes it self-sustaining and carbon-neutral. However, the release of hydrogen from formic acid demands selective catalytic decomposition since the generation of CO by dehydration pathway has an adverse effect (catalyst poisoning) in fuel cell's performance [9–11].

$$HCOOH \leftrightarrow H_2 + CO_2 \quad \Delta G = -48.4\,\text{kJ mol}^{-1} \text{ (Dehydrogenation)},$$

$$HCOOH \leftrightarrow H_2O + CO \quad \Delta G = -28.5\,\text{kJ mol}^{-1} \text{ (Dehydration)}.$$

Several ruthenium-based homogeneous catalysts have shown promising results towards dehydrogenation of formic acid, but heterogeneous catalysts, owing to the ease of separation, recycling and room temperature operation have currently gained the focus of researchers [12–15]. Supported metal catalysts containing Pd, Pt, Ir, Ru and Au nanoparticles were shown to completely decompose HCOOH with 97% selectivity for hydrogen at high temperatures (450–500 K), contrary to only 10% conversion at low temperatures (298–350 K) [16–18]. On the other hand,

This article is part of the Topical Collection: SAMat Focus Issue.

Electronic supplementary material: The online version of this article (https://doi.org/10.1007/s12034-020-02295-0) contains supplementary material, which is available to authorized users.

Published online: 21 November 2020

formic acid in presence of sodium formate was reported to show 100% conversion and selectivity at 333 K, indicating the importance of formate ion in formic acid decomposition at near ambient conditions [19–21]. In addition to sodium formate, other additives like amines and Brønsted bases were also employed to promote the dehydrogenation process [22,23]. Recent trends in the design of catalyst support, give much emphasis for the incorporation of basic moities favourable for deprotonation of HCOOH [24,25]. In this regard, graphene oxide (GO), being a robust material, at low pH, provides various functional moieties like –COOH, C=O and C–OH for facile incorporation of basic functionality [26,27]. Moreover, 2D GO layers enable easy access of HCOOH molecules to the active sites on exfoliation. There are few reports on amine-functionalized GO support, however, they demand large amount of palladium content (about 20 wt%) and/or additional sodium formate for better efficiency [15,28–32]. The necessity of sodium formate in presence of amine-functionalization is not clear. Therefore, it is necessary to have a better understanding about the amine-functionalized GO systems to minimize the usage of Pd for dehydrogenation of formic acid without the addition of external formate ions at room temperature.

Hence, in this work, we have investigated palladium-loaded amino silane-functionalized GO catalytic system for formic acid decomposition at room temperature. We found that the best performing catalyst having low Pd content ($\sim$5 wt%) requires about 40 wt% amino silane functionalization on the GO support. Additionally, it was noticed that the inconsequential interaction of evolved gaseous product (CO_2) with catalyst, played a significant role in catalyst's recyclability.

2. Experimental

2.1 *Materials and methods*

Formic acid (HCOOH) (Merck, AR, 98–100%), graphite powder (20 μm) (Sigma Aldrich), H_2SO_4 (AR, 98%), $NaNO_3$ (Sigma Aldrich), $KMnO_4$ (S D Fine Chemicals), H_2O_2 (Merck, 30%), (3-aminopropyl)triethoxysilane (APTES) (Sigma Aldrich, 99%), K_2PdCl_4 (Sigma Aldrich, 99% trace metals basis), $NaBH_4$ (S D Fine Chemicals), n-propylamine (Sigma Aldrich, 98%), ninhydrin (Sigma Aldrich), LiOH (Sigma Aldrich), glacial acetic acid (S D Fine Chemicals), hydrindantin dihydrate (Sigma Aldrich) were used without any further purification. Deionized water with specific resistance of 18.2 MΩ cm was used for all experiments.

2.2 *Synthesis of materials for formic acid decomposition*

2.2a *Synthesis of GO:* GO was prepared according to Hummer's method [33]. Graphite (1 g), $NaNO_3$ (0.5 g) and concentrated H_2SO_4 (23 ml) were thoroughly mixed in a 250 ml round bottom flask at 273 K (ice bath). To this, $KMnO_4$ (3 g) was added slowly in small portions under vigorous stirring. Temperature was maintained below 293 K during this time. Thereafter, ice bath was removed and the reaction mixture was stirred at room temperature for 30 min. To this, 46 ml of water was added slowly to give violet effervescence and brown coloured suspension. Thereafter, the temperature was raised to 353 K and 140 ml of hot water was added to it. It was kept at that temperature for 15 min and then cooled. Finally, 10 ml of 30% H_2O_2 was added to the slurry to reduce unreacted permanganate. Thus, the straw-yellow colour mixture obtained was centrifuged at 5000 rpm and washed several times with distilled water until the pH turned neutral. Then, the precipitate was lyophilized to get GO powder.

2.2b *Synthesis of Pd/rGO-AP-based catalyst:* To prepare amino silane functionalized GO with weight ratio of GO:APTES as 1:1, firstly 200 mg of GO was dispersed in 60 ml of water for 20 min. Then, 211 μl (200 mg) of APTES was added to it in dropwise manner under vigorous stirring. The mixture was stirred for 48 h and separated by centrifugation [34]. The precipitate obtained was the functionalized GO which was washed multiple times with water and ethanol and dried. Other weight ratios of GO:APTES, 2:1 and 1:2 were also prepared in similar way by varying the quantity of APTES. The terminology, rGO-AP is specifically used in this paper for amine-functionalized GO with the weight ratio of GO:APTES as 1:1.

Palladium nanoparticles were synthesized on rGO-AP by dispersing 100 mg of it in 50 ml of water followed by the addition of 472 μl of 0.1 M K_2PdCl_4. The mixture was stirred for 30 min and, 2 ml of 0.1 M $NaBH_4$ solution was quickly added. Thereafter, it was stirred for 30 min more and then, centrifuged at 10,000 rpm [35]. The precipitate obtained was washed with water, ethanol and dried to obtain 5 wt% palladium-loaded rGO-AP as catalyst. Additionally, 1, 3 and 10 wt% of palladium were also synthesized on rGO-AP, following the same protocol. In this report, the term Pd/rGO-AP is specifically used for catalyst containing 5 wt% Pd on 1:1 weight ratio of GO:APTES unless otherwise mentioned.

Pd/rGO was also prepared by the same protocol using rGO support.

2.3 *Formic acid decomposition*

Formic acid decomposition was performed in an air-tight customized set-up (supplementary figure S1) consisting of two-necked round bottom flask (25 ml) in which one of the necks was modified with a stopper and attached to a 250 ml graduated burette filled with water. The burette was used to monitor the volume of gas evolved from formic acid decomposition through downward displacement of water.

Additionally, a levelling bulb was connected to the burette to maintain constant pressure (1 atm) throughout the catalysis. For catalytic study, 50 mg catalyst dispersed in 9 ml of water was added to the reaction vessel and tightly sealed to have a closed system. Then, 1 ml of HCOOH (10 M) was injected into the catalyst dispersion under stirring. Thereafter, formic acid decomposition was evaluated from the total gas evolution at different time intervals which was collected in the burette and analysed by gas chromatography.

2.4 *TOF*

Initial turnover frequency (TOF) was calculated by considering the total amount of gas evolved from formic acid decomposition in 30 min using the following equation:

$$\text{TOF} = \frac{\text{Total volume of gas evolved in 30 min (ml)}}{2 \times 24.81 \times (\text{moles of Pd}) \times \text{time (h)}}\ \text{h}^{-1}.$$

2.5 *Characterizations*

Powder X-ray diffraction (PXRD) patterns were recorded in Rigaku diffractometer with CuKα radiation (λ = 1.54 Å). FTIR spectra were recorded on Bruker IFS 66 v/S spectrometer. TEM images were obtained from TECNAI T20 operating at an acceleration voltage of 100 kV. Inductive coupled plasma-optical emission spectroscopy (ICP-OES) was carried out in Perkin-Elmer Optima 7000 DV. Thermogravimetric analysis (TGA) was performed using Mettler Toledo 850 from 30 to 1000°C in oxygen atmosphere with heating rate at 10°C min^{-1}. Gas analysis was done by gas chromatography using Perkin Elmer, Clarus 580 GC equipped with TCD detector and a methanator with a detection limit of CO below 10 ppm.

3. Results and discussion

3.1 *Characterization of Pd/rGO-AP (5 wt% Pd, GO:APTES weight ratio 1:1)*

The catalyst was synthesized in a step-wise manner according to scheme 1. Firstly, the as prepared GO was allowed to interact with APTES to form amino silane-functionalized reduced-graphene oxide (rGO-AP). The PXRD pattern of pristine and APTES modified GO are

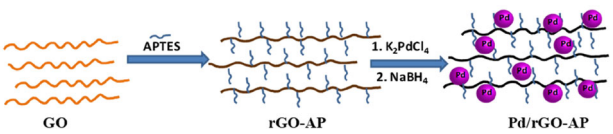

Scheme 1. Step-wise synthesis of Pd/rGO-AP catalyst.

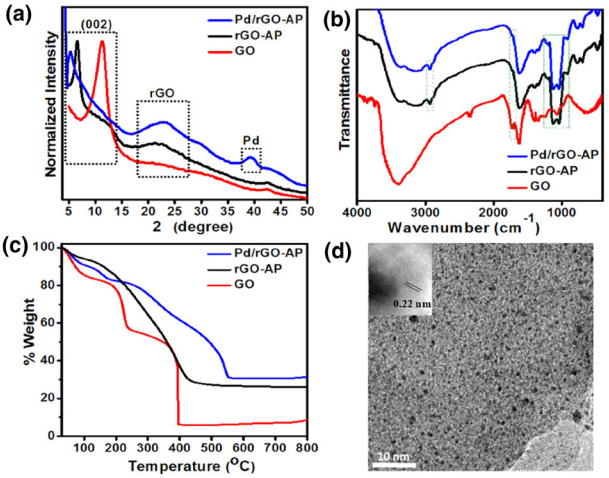

Figure 1. Characterization of GO, rGO-AP and Pd/rGO-AP by (**a**) PXRD, (**b**) FTIR, (**c**) TGA and (**d**) TEM (inset shows the interlayer distance of Pd (111) plane).

shown in figure 1a. Introduction of APTES in GO resulted in the increase of interlayer spacing as evident from the shifting of peak at 2θ = 11.3°, associated with pure GO to a lower angle 6.5° in case of rGO-AP (figure 1a). This increase in *d*-spacing is significant considering the fact that GO underwent reduction to rGO during this process (corresponding peak at 2θ = 23° for rGO-AP, figure 1a) and therefore, the interlayer spacing was expected to be lower than that of GO. The absence of C=O stretch (1734 cm^{-1}) in the FTIR spectrum of rGO-AP (figure 1b) confirmed the reduction of GO to rGO upon addition of amino silane. Further, borohydride reduction of palladium precursor (K_2PdCl_4) in the presence of rGO-AP composite provided Pd/rGO-AP catalyst (scheme 1). The presence of palladium in the catalyst was evident from its PXRD (figure 1a), where the peak at 39.3° was assigned for Pd (111) (JCPDS 05-0681). The FTIR spectra (figure 1b) of both rGO-AP and Pd/rGO-AP show characteristic peaks at 2932 cm^{-1} (sp^3 C–H) and 3148 cm^{-1} (N–H stretch) associated with the aminopropyl moities of APTES. The additional peaks observed at 1040 and 1130 cm^{-1} corresponding to Si–O–C and Si–O–Si stretches, respectively, suggest that the silylation of GO with APTES probably occurs through Si-OEt functional groups [27,36]. Ninhydrin test performed over Pd/rGO-AP to quantify the primary amine, further confirmed the presence of free amine groups (of APTES) in significant amount (1 mmol g^{-1}) [37]. ICP-OES analysis showed the Pd content was 5 wt% in Pd/rGO-AP. Thermogravimetric analysis (figure 1c) performed under oxygen atmosphere showed 20% extra residual weight for rGO-AP as compared to GO due to the formation of silica upon combustion of APTES. This residual silica corresponds to 40 wt% of APTES in rGO-AP. The TEM image in figure 1d displayed the uniform distribution of palladium nanoparticles on rGO-AP sheet with an average particle diameter of 1.5 nm. It is to be noted that even after borohydride

reduction step, Pd/rGO-AP was well exfoliable in aqueous medium owing to charge repulsion generated by the protonated amine groups [38].

3.2 *Formic acid decomposition*

Catalytic decomposition of formic acid was carried out in a leak-free reactor as shown in supplementary figure S1. The results in figure 2a present the effect of amine functionalization on GO for catalytic activity with 5 wt% palladium loading. It was observed that the rate of formic acid decomposition was negligible (0.4 ml gas evolved in 30 min) in case of catalyst using only rGO as support compared to APTES-functionalized rGO (GO:APTES, 2:1), where a large amount (60 ml) of gas was liberated in the same period of time. Moreover, increasing the amount of APTES in the catalyst, improved the catalytic activity until it reached 50 wt% with respect to rGO (figure 2a).

Variations of palladium loading on rGO-AP composite (GO:APTES, 1:1) were also studied for formic acid decomposition as shown in figure 2b. A significant enhancement in the initial rate of decomposition was observed from 0.56 to 4 ml min^{-1} by increasing the palladium content from 1 to 3 wt%. Further increase in palladium content improved the decomposition rate to 6 and 7 ml min^{-1} for 5 and 10 wt%, respectively. Of all the compositions, Pd/rGO-AP catalyst with 5 wt% palladium and 1:1 weight ratio of GO:APTES exhibited the best results for complete formic acid decomposition at room temperature with TOF of 477 h^{-1}. Further, analysis of gaseous products obtained using gas chromatography confirmed the presence of only carbon dioxide and hydrogen.

On completion of first run, addition of formic acid (1 ml, 10 M) to the catalyst (Pd/rGO-AP) dispersion showed a drastic decrease in the rate of evolution of gases from 5 to 1.2 ml min^{-1} (figure 3a, process 1 in scheme 2). On the other hand, when the dehydrogenation was carried out over the catalyst separated (and washed with water) after first run, no significant decrease in activity was observed (figure 3b, process 2 in scheme 2). This negates the possibility of CO poisoning for the initial loss of activity observed in figure 3a [39,40]. Repeating the catalytic run for the third and fourth cycles, however, showed 45% decrease in activity even after washing the catalyst prior to each cycle (figure 3b). These observations necessitated us to consider the unavailability of free amine functionality (facilitates the formation of formate ion) due to its interaction with carbon dioxide evolved during catalytic reaction. It is because, after complete decomposition of HCOOH, only catalyst dispersion in aqueous medium remains in equilibrium with gaseous products. Moreover, it is well known that amines under ambient conditions absorbs CO_2 to form stable CO_2–amine complex (carbamates, ammonium bicarbonate, etc.), which in presence of excess water undergoes hydrolysis to provide free amine [41]. Therefore, it could be expected that removal of gases which are generally collected in the burette will decrease the contact time of carbon dioxide with amine groups present in the catalyst. Thus, allowing the gaseous products (CO_2 and H_2) to leave the reaction chamber followed by washing the catalyst in each cycle (process 3 in scheme 2) extended the performance of the catalyst up to four cycles (figure 3c). It was further verified by control experiments in which fresh catalyst (aqueous dispersion) was pre-equilibrated (for 12 h) with carbon dioxide gas in one case and mixture of carbon dioxide and hydrogen gas (gaseous product from HCOOH decomposition) in other case before addition of formic acid. A 40% decrease in decomposition rate of formic acid was observed in both the cases of pre-equilibrated catalysts as compared to the untreated one (figure 3d). This confirmed the loss in catalytic activity of Pd/rGO-AP in presence of carbon dioxide.

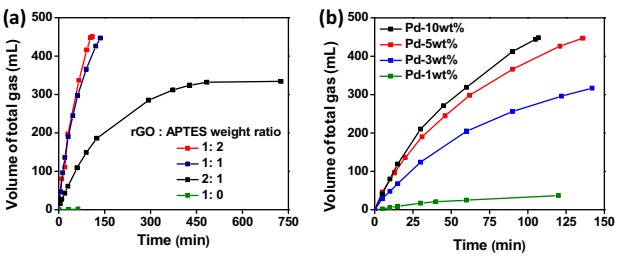

Figure 2. HCOOH decomposition at room temperature with (**a**) 5 wt% palladium loaded on different APTES-functionalized GO support and (**b**) rGO:APTES (1:1) as support by varying the palladium content. All the experiments were performed with 10 ml, 1 M HCOOH and 50 mg catalyst ($n_{Pd}/n_{HCOOH} = 0.002$).

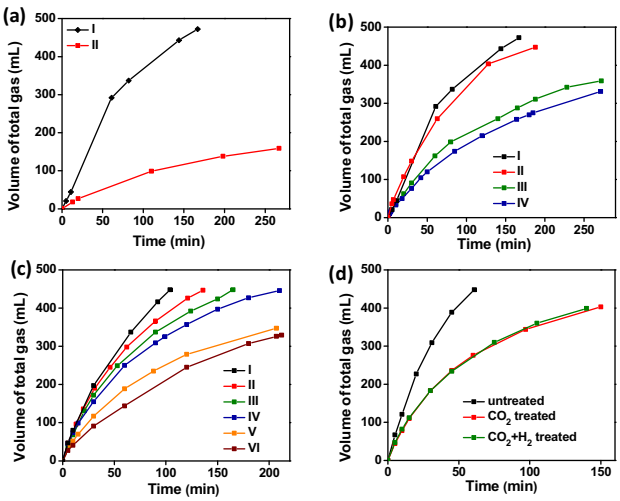

Figure 3. Recyclability of Pd/rGO-AP catalyst for HCOOH dehydrogenation. Cases in which gaseous products were collected in burette and catalyst underwent (**a**) no treatment, (**b**) separation and washing with water before every cycle, (**c**) gaseous products are constantly removed from the system followed by catalyst separation and washing in each cycle and (**d**) compares formic acid decomposition by pre-treated Pd/rGO-AP with CO_2 and (CO_2 + H_2) gas with untreated catalyst.

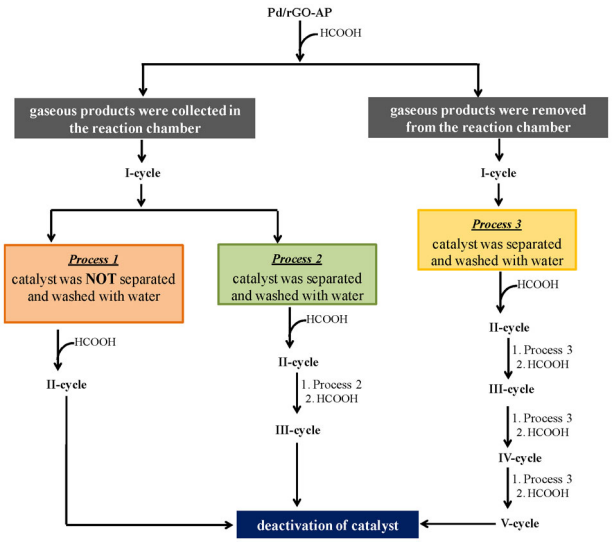

Scheme 2. Summarizes the recyclability of Pd/rGO-AP catalyst for HCOOH decomposition.

Aliquots of the reaction mixture (without catalyst) were analysed for Pd and APTES after every cycle to understand the loss in catalytic activity in fifth and sixth cycles (figure 3c). Palladium concentration in the aliquots was found to be <0.5 ppm from ICP-OES, suggesting retention of palladium in the catalyst. However, the average particle size of palladium increased from 1.5 nm in the first cycle to 4.2 nm after fifth cycle (supplementary figure S3). This observation can be attributed to the leaching of APTES moieties (serve as anchoring sites) during every cycle of formic acid decomposition as quantified by the Ninhydrin test (supplementary table S1) [42]. Therefore, the decrease in APTES functionality due to leaching and increase in size of palladium nanoparticles collectively accounted for the irreversible decrease in catalytic activity beyond fourth cycle.

4. Conclusions

Pd/rGO-APTES catalyst with relatively low amount of palladium (5 wt%) showed good activity for additive-free formic acid decomposition to give hydrogen at room temperature. The interaction of evolved CO_2 with the amino silane moieties had a negative influence on the activity of the catalyst. So, the constant removal of gaseous products from reaction chamber played a vital role in retaining the catalytic activity to some extent. Although the presence of amino silane showed enhanced activity for formic acid dehydrogenation, their poor stability in acidic environment (for a longer period of time), as well as their strong interaction with CO_2 diminishes the potential of Pd/rGO-AP to be used as an effective catalyst.

Acknowledgements

We thank Prof C N R Rao, FRS, for his constant support and inspiration. Funding from DSTJNCASR Nanomission Project (SR/NM/TP-25/2016) by Government of India are greatly acknowledged. SSB thanks JNCASR for research facilities and fellowship. MST and EA thank JNCASR for summer research program (POCE and SRFP). ME thanks Sheikh Saqr Career Award Fellowship.

References

[1] Jacobson M Z, Colella W and Golden D 2005 *Science* **308** 1901
[2] Aceves S M, Martinez-Frias J and Garcia-Villazana O 2000 *Int. J. Hydrog. Energy* **25** 1075
[3] Orimo S-I, Nakamori Y, Eliseo J R, Züttel A and Jensen C M 2007 *Chem. Rev.* **107** 4111
[4] Furukawa H, Ko N, Go Y B, Aratani N, Choi S B, Choi E *et al* 2010 *Science* **329** 424
[5] Yang S J, Kim T, Im J H, Kim Y S, Lee K, Jung H *et al* 2012 *Chem. Mater.* **24** 464
[6] Hodoshima S, Takaiwa S, Shono A, Satoh K and Saito Y 2005 *Appl. Catal. A: Gen.* **283** 235
[7] Kariya N, Fukuoka A and Ichikawa M 2002 *Appl. Catal. A: Gen.* **233** 91
[8] Preuster P, Papp C and Wasserscheid P 2016 *Acc. Chem. Res.* **50** 74
[9] Tingelöf T, Hedström L, Holmström N, Alvfors P and Lindbergh G 2008 *Int. J. Hydrog. Energy* **33** 2064
[10] Loges B, Boddien A, Gärtner F, Junge H and Beller M 2010 *Top. Catal.* **53** 902
[11] Johnson T C, Morris D J and Wills M 2010 *Chem. Soc. Rev.* **39** 81
[12] Fellay C, Dyson P J and Laurenczy G 2008 *Angew. Chem. Int. Ed.* **47** 3966
[13] Grasemann M and Laurenczy G 2012 *Energy Environ. Sci.* **5** 9698
[14] Kiss F E, Jovanović M and Bošković G C 2010 *Fuel Process. Technol.* **91** 1316
[15] Liu H, Huang B, Zhou J, Wang K, Yu Y, Yang W *et al* 2018 *J. Mater. Chem. A* **6** 1979
[16] Fukuda K, Noto Y, Onishi T and Tamaru K 1967 *T. Faraday Soc.* **63** 3072
[17] Gazsi A, Bánsági T and Solymosi F 2011 *J. Phys. Chem. C* **115** 15459
[18] Solymosi F, Koós Á, Liliom N and Ugrai I 2011 *J. Catal.* **279** 213
[19] Zhu Q-L, Tsumori N and Xu Q 2014 *Chem. Sci.* **5** 195
[20] Wang Z-L, Yan J-M, Wang H-L, Ping Y and Jiang Q 2012 *Sci. Rep.* **2** 598
[21] Wan C, Yao F, Li X, Hu K, Ye M, Xu L *et al* 2016 *Chem. Select.* **1** 6907
[22] Outka D A and Madix R 1987 *Surf. Sci.* **179** 361
[23] Bi Q-Y, Du X L, Liu Y-M, Cao Y, He H-Y and Fan K-N 2012 *J. Am. Chem. Soc.* **134** 8926

[24] Navlani-García M, Mori K, Salinas-Torres D, Kuwahara Y and Yamashita H 2019 *Front. Mater.* **6** 2213
[25] Wang X, Meng Q, Gao L, Jin Z, Ge J, Liu C *et al* 2018 *Int. J. Hydrog. Energy* **43** 7055
[26] Shih C-J, Lin S, Sharma R, Strano M S and Blankschtein D 2012 *Langmuir* **28** 235
[27] Abbas S S, Rees G J, Kelly N L, Dancer C E J, Hanna J V and McNally T 2018 *Nanoscale* **10** 16231
[28] Wang Z, Hao X, Hu D, Li L, Song X, Zhang W *et al* 2017 *Catal. Sci. Technol.* **7** 2213
[29] Wang Z-L, Yan J-M, Wang H-L, Ping Y and Jiang Q 2013 *J. Mater. Chem. A* **1** 12721
[30] Hosseini H, Mahyari M, Bagheri A and Shaabani A 2014 *J. Power Sources* **247** 70
[31] Song F-Z, Zhu Q-L, Tsumori N and Xu Q 2015 *ACS Catal.* **5** 5141
[32] Yan J M, Li S J, Yi S S, Wulan B R, Zheng W T and Jiang Q 2018 *Adv. Mater.* **30** 1703038
[33] Hummers W S Jr and Offeman R E 1958 *J. Am. Chem. Soc.* **80** 1339
[34] Serna-Guerrero R, Da'na E and Sayari A 2008 *Ind. Eng. Chem. Res.* **47** 9406
[35] Krishna K S, Sandeep C S, Philip R and Eswaramoorthy M 2010 *ACS Nano* **4** 2681
[36] Hou S, Su S, Kasner M L, Shah P, Patel K and Madarang C J 2010 *Chem. Phys. Lett.* **501** 68
[37] Sun S-W, Lin Y-C, Weng Y-M and Chen M-J 2006 *J. Food Compos. Anal.* **19** 112
[38] Achari A, Datta K, De M, Dravid V P and Eswaramoorthy M 2013 *Nanoscale* **5** 5316
[39] Croft G and Fuller M 1977 *Nature* **269** 585
[40] Jiang K, Xu K, Zou S and Cai W-B 2014 *J. Am. Chem. Soc.* **136** 4861
[41] Böttinger W, Maiwald M and Hasse H 2008 *Fluid Phase Equilib.* **263** 131
[42] Moreno M, Ibañez F J, Jasinski J B and Zamborini F P 2011 *J. Am. Chem. Soc.* **133** 4389